Large Magnetic Anisotropy in Pentacoordinate Ni^{II} Complexes

Jean-Noël Rebilly,[a] Gaëlle Charron,[a] Eric Rivière,[a] Régis Guillot,[a] Anne-Laure Barra,[b] Marc Durán Serrano,[c] Joris van Slageren,[c] and Talal Mallah*[a]

Abstract: Pentacoordinate complexes in which Ni^{II} is chelated by the tridentate macrocyclic ligand 1,4,7-triisopropyl-1,4,7-triazacyclononane (*i*Prtacn) of formula [Ni(*i*Prtacn)X$_2$] (X = Cl, Br, NCS) have relatively large magnetic anisotropies, revealed by the large zero-field splitting (zfs) axial parameters |D| of around 15 cm^{-1} measured by frequency-domain magnetic resonance spectroscopy (FDMRS) and high-field high-frequency electron paramagnetic resonance (HF-HFEPR). The spin Hamiltonian parameters for the three complexes were determined by analyzing the FDMRS spectra at different temperatures in zero applied magnetic field in an energy window between 0 and 40 cm^{-1}. The same parameters were determined from analysis of HF-HFEPR data measured at different frequencies (285, 380, and 475 GHz) and at 7 and 17 K. The spin Hamiltonian parameters D (axial) and E (rhombic) were calculated for the three complexes in the framework of the angular overlap model (AOM). The nature and magnitude of the magnetic anisotropy of the three complexes and the origin of the influence of the X atoms were analyzed by performing systematic calculations on model complexes.

Keywords: EPR spectroscopy · macrocyclic ligands · magnetic properties · N ligands · nickel

Introduction

Magnetic anisotropy is a very important property of magnetic systems that shapes their magnetic behavior; the blocking temperatures of magnetic systems based on coordination compounds (magnetic coordination nanoparticles, single-molecule magnets, single-chain magnets) are controlled at the microscopic level by the anisotropy of the single metal ions.[1] Ni^{II} is a versatile metal ion able to coordinate four, five, or six atoms in different geometries. Within the formalism of crystal-field theory, the ground spectroscopic term (^{3}A$_2$) of hexacoordinate Ni^{II} complexes with strictly O_h symmetry is triply degenerate and this degeneracy cannot be lifted by spin–orbit coupling (the three $M_S = 0$ and ± 1 sublevels of the $S = 1$ spin state are pure and have the same energy) and hence magnetic anisotropy is absent. When the symmetry is lower than O_h and the ground term is orbitally nondegenerate, it can be shown that the orbital degeneracy of the excited states is lifted. Coupling between the ground term and the excited terms via the spin–orbit operator (second-order spin–orbit coupling) leads to a situation in which the three spin sublevels ($M_S = 0, \pm 1$) no longer have the same energy; this form of magnetic anisotropy, known as zero-field splitting (ZFS), is expressed by the D and E parameters of the spin Hamiltonian.[2] Thus, in the case of hexacoordinate complexes which have symmetry lower than O_h and a ground term with no first-order spin–orbit coupling, the magnitude of the magnetic anisotropy depends mainly on two parameters: 1) the energy difference between the ground and excited terms Δ_i and 2) the degree of splitting of the excited terms δ_j.[3] To induce a large magnetic anisotropy (i.e., large D value), Δ_i must be small and δ_j must be large. For hexacoordinate Ni^{II} complexes, it is very difficult to act on Δ_i, which is generally larger than 10000 cm^{-1}; δ_j, which depends on the amount of distortion, can be more easily controlled by introducing chelating ligands (geometrical distortion) and/or by inducing dissymmetry in the coordination sphere of the metal ion by simultaneous use of pure σ-donating and σ/π-donating ligands (electronic distortion), for

[a] Dr. J.-N. Rebilly, G. Charron, Dr. E. Rivière, Dr. R. Guillot, Prof. T. Mallah
Institut de Chimie Moléculaire et des Matériaux d'Orsay
CNRS, Université Paris 11
91405 Orsay Cedex (France)
E-mail: mallah@icmo.u-psud.fr

[b] Dr. A.-L. Barra
Laboratoire des Champs Magnétiques Intenses, UPR CNRS 5021
25, avenue des Martyrs, B.P. 166, 38042 Grenoble Cedex 9 (France)

[c] Dr. M. D. Serrano, Dr. J. van Slageren
1. Physikalisches Institut, Universität Stuttgart
Pfaffenwaldring 57, 70550 Stuttgart (Germany)

Supporting information for this article is available on the WWW under http://www.chemeurj.org/ or from the author.

example. However, apart from a few exceptions, splitting of the M_S sublevels is scarcely larger than a few wavenumbers.[4] A simple way to decrease Δ_i is to reduce the number of ligands around the metal ion. This has the effect of increasing the value of δ_i, since the symmetry is reduced on going from hexacoordinate to penta- or tetracoordinate complexes and thus, everything being equal, of increasing the magnitude of the magnetic anisotropy. Tetracoordinate complexes of formula [Ni(PPh$_3$)$_2$X$_2$] and [Tp*NiX] (where Tp* is the tridentate hydrotris(3,5-dimethylpyrazolyl)borate and X=Cl, Br, I) have been studied, and large magnetic anisotropies have been found.[5] Unfortunately, the [Ni-(PPh$_3$)$_2$X$_2$] complexes cannot be used as building blocks in coordination systems since substitution reactions with other ligands will deeply affect their electronic structure and thus their magnetic anisotropy. The [Tp*NiX] complexes are more suitable for this purpose thanks to the presence of the chelating Tp* ligand, which is not easily substituted by other ligands. However, a thorough study on these complexes showed that their magnetic anisotropy is highly dependent on the nature of the substitutable X ligand.

An alternative approach consists of using pentacoordinate complexes, which, to the best of our knowledge, have not been explored for their magnetic anisotropy behavior yet. Pentacoordinate Ni^{II} complexes can span the geometries between square-pyramidal (SPy) and trigonal-bipyramidal (TBP). The SPy complexes are expected to have a non-negligible anisotropy, while TBP species are expected to have a huge magnetic anisotropy because their D_{3h} symmetry leads to an orbitally degenerate ground spectroscopic term (^{3}E) in which first order spin–orbit coupling occurs.

Here we show that the tridentate macrocyclic ligand 1,4,7-triisopropyl-1,4,7-triazacyclononane (iPrtacn) leads on reaction with Ni^{II} salts to pentacoordinate complexes of formula [Ni(iPrtacn)X$_2$] (X=Cl, Br, NCS). The presence of the three bulky isopropyl groups precludes the formation of hexacoordinate complexes of the types [Ni(iPrtacn)$_2$]$^{2+}$ or [Ni(iPrtacn)X$_3$]$^-$ (X=Cl, Br, I) and thus stabilizes pentacoordination. Furthermore, the macrocyclic nature of the ligand bestows considerable thermodynamic stability on the Ni(iPrtacn) moiety that fixes its structural parameters with respect to substitution of the X ligand. The structures of the three complexes were solved and their magnetic properties were studied by routine magnetization measurements. The axial and rhombic magnetic anisotropy parameters **D** and **E** corresponding to the spin Hamiltonian $H = D(S_z^2 - S(S+1)/3) + E(S_x^2 - S_y^2)$ were determined by high-frequency high-field electron paramagnetic resonance (HF-HFEPR) and frequency-domain magnetic resonance spectroscopy (FDMRS). The experimental spin Hamiltonian parameters were analyzed and rationalized by using the angular overlap model (AOM).

Results and Discussion

Synthesis and crystal structures: Syntheses of the iPrtacn ligand and [Ni(iPrtacn)Cl$_2$] (**1**) can be found elsewhere.[6]

[Ni(iPrtacn)Br$_2$] (**2**) was prepared by the same procedure as for **1** by using NiBr$_2$·6H$_2$O. [Ni(iPrtacn)(NCS)$_2$] (**3**) was prepared from **2** (see Experimental Section). Microcrystalline solids were obtained for the three complexes in yields exceeding 70% based on metal content. These solids were subsequently used for all the magnetic studies. Single crystals of the chloride and bromide complexes were obtained by diffusion of THF into a methanolic solution of the parent complex. Single crystals of [Ni(iPrtacn)(NCS)$_2$] were obtained by mixing equimolar methanolic solutions of [Ni(iPrtacn)Br$_2$] and NaNCS and leaving the mixture to stand undisturbed for two hours. The structures of the three complexes are very similar; the Ni atom is pentacoordinate and is surrounded by the three nitrogen atoms (N1–N3) of iPrtacn and two X atoms (Figure 1 and Figure S1 a,b in the

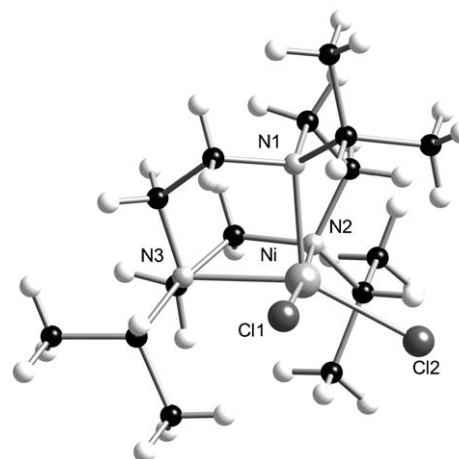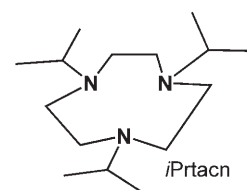
Figure 1. View of the molecular structure of **1**.

Supporting Information). The molecular structure can be described as a distorted square pyramid,[7] the base of which is formed by N2 and N3 of iPrtacn and X1 and X2, while the third nitrogen atom N1 of the organic ligand occupies the apical position. The four atoms Ni, N2, N3, and X1 belong to the same plane with X1N3N2Ni dihedral angles of 1.04, 0.44, and 0.53° for **1**, **2**, and **3** respectively. The N2-Ni-N3 bite angles of iPrtacn within this plane are almost the same for the three complexes and vary between 81.8 and 83.5°, while the N1-Ni-N2 and N1-Ni-N3 bite angles are close to 86° for the three complexes. The N1-Ni-X1 angles are around 93°. The N3-Ni-X1 angles are around 94.5° for the three complexes, and the N2-Ni-X1 angles are almost linear. The apical Ni−N1 bond length (2.08 Å) varies by less

than 0.01 Å among the three complexes. Distortion from SPy geometry comes from the position of the X2 atoms; the N1-Ni-X2 angles are far from the 90° which would correspond to SPy geometry. These angles are 121.5, 118.2, and 121.4° for **1**, **2**, and **3** respectively. Complex **2** has one important difference to **1** and **3**, that is, the N1-Ni-X2 angle, which is smaller for **2** (118.2°) than for **1** and **3** (121.5°). Another difference is that the shortest bond length corresponds to the atom occupying the apical position (N1) for **1** and **2**, while it is the equatorial Ni−N2$_{NCS}$ bond in **3**.

A space-filling drawing of complex **1** shows clearly that the *i*Prtacn ligand acts as a cap on the metal ion that prevents approach of more than two other monodentate ligands (Figure 2). The position of the two X ligands around the
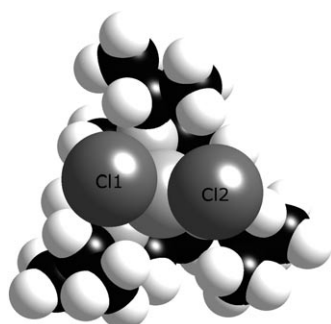

Figure 2. Space-filling view of the molecular structure of **1** showing the steric hindrance imposed by the *i*Prtacn ligand.

metal ion is imposed to a certain extent by the presence of the bulky isopropyl groups, and this leads to the observed distortion from SPy geometry. Further distortion from SPy geometry by increasing the N1-Ni-X2 angle to 135° would lead to a geometry close to that of a distorted TBP with the N2-Ni-X1 axis as the pseudo-trigonal axis. However, such an increase of the N1-Ni-X2 angle cannot take place without a major change in the conformation of the organic ligand, which is unlikely to occur.

Magnetization studies: To gain preliminary insight into the magnetic behavior of the complexes, routine magnetization studies [$M = f(\mu_0 H)$] at different temperatures were carried out. Then, the data were fitted by full diagonalization of the energy matrices for 120 orientations of each value of magnetic field by means of a homemade software based on the following spin Hamiltonian: $H = \mu_B S \cdot g \cdot B + D[S_z^2 - S(S+1)/3] + E(S_x^2 - S_y^2)$, where the first term is the Zeeman effect,

and the second and the third terms express the axial and rhombic anisotropy, respectively. The fit procedure was repeated several times starting from different values for g, D, and E. For the Zeeman effect, only an isotropic g value was taken into account. The fits were carried out simultaneously at several temperatures for each complex, and the parameters were extracted with agreement factors on the order of 10^{-5} (Figure 3 and Figure S2 a,b in the Supporting Information). The values of the three parameters g, D, and E for
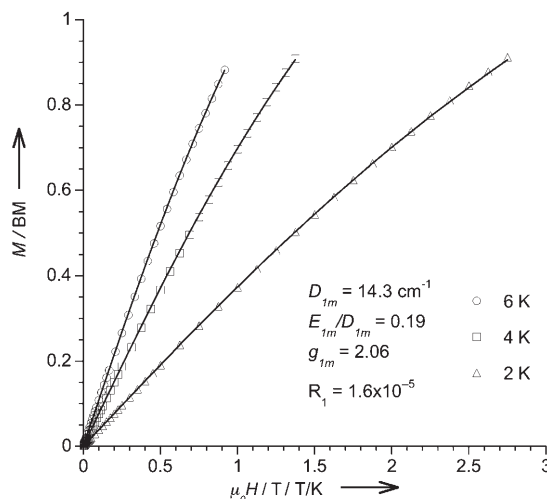

Figure 3. $M = f(\mu_0 H/T)$ at $T = 2$ K ($\triangle$), 4 K ($\square$) and 6 K ($\circ$) for **1**.

each complex corresponding to the best fits are (see Table 1): $g_{1m} = 2.06$, $D_{1m} = 14.3$ cm^{-1}, $E_{1m} = 2.7$ cm^{-1} ($E_{1m}/D_{1m} = 0.19$); $g_{2m} = 2.13$, $D_{2m} = 11.0$ cm^{-1}, $E_{2m} = 0$ cm^{-1} ($E_{2m}/D_{2m} = 0$); and $g_{3m} = 2.2$, $D_{3m} = 13.8$ cm^{-1}, $E_{3m} = 4.0$ cm^{-1} ($E_{3m}/D_{3m} = 0.29$), where the subscript m indicates that these parameters were derived from magnetization measurements). The sign of D was found to be positive and no reasonable fit could be obtained when imposing negative D values for any of the complexes, although for complex **3** the sign of D has almost no meaning due to its large rhombicity.

FDMRS studies: One of the most direct techniques to evaluate quite accurately the ZFS parameters of the spin Hamiltonian is FDMRS.[8] The spectra of the three complexes were recorded in the 0–40 cm^{-1} energy range between 1.8 and 50 K in zero applied magnetic field. For **1**, two lines are observed at $e_1 = (12.7 \pm 0.2)$ and $e_2 = (19.1 \pm 0.1)$ cm^{-1} (Figure 4). This is the signature of splitting of the $S = 1$ spin

Table 1. Experimental data for the spin Hamiltonian parameters obtained from the three different techniques.

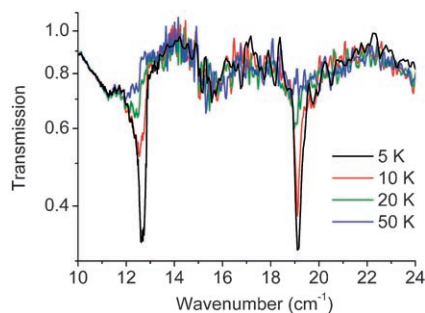|	Magnetization			FDMRS		HF-HFEPR				
	D_m [cm^{-1}]	E_m/D_m	g_m	D_F [cm^{-1}]	E_F/D_F	D_E [cm^{-1}]	E_E/D_E	g_x	g_y	g_z
1 (X=Cl)	14.0	0.19	2.06	15.9	0.20	15.70	0.216	2.10	2.05	2.15
						15.80	0.202	2.12	2.05	2.15
2 (X=Br)	11.0	0	2.13	13.8	0.24	13.93	0.25	2.13	2.00	2.00
3 (X=*N*CS)	13.8	0.29	2.20	15.9	0.31	16.12	0.324	2.25	2.22	2.23
						16.35	0.319	2.25	2.22	2.23

Figure 4. FDMRS spectra of **1** at various temperatures.

state into its three components described by the wave functions $|0\rangle$, $|1\rangle_A$ ($|1\rangle-|-1\rangle$), and $|1\rangle_S$ ($|1\rangle+|-1\rangle$) in order of increasing energy. The temperature-dependence studies showed an increase in the intensity of the two bands on cooling, which indicates that the two transitions occur from a ground level to two excited ones. Since the selection rules impose $\Delta M_S = \pm 1$, the ground level is then $M_S = 0$. This leads to the energy levels depicted in Scheme 1.
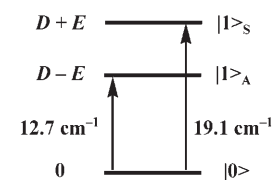
Scheme 1. Energy levels in **1**.

When the ground level is $M_S = 0$, the axial zfs parameter D is considered to be positive and the following values can be extracted from the experimental data (see Table 1): $E_{1F} = (e_2-e_1)/2 = 3.2$ cm^{-1} and $D_{1F} = (e_2+e_1)/2 = 15.9$ cm^{-1} ($E_{1F}/D_{1F} = 0.20$). The other two complexes have similar spectra with two lines as well (see Figure S3a,b in the Supporting Information). The same temperature dependence was found, that is, D is positive for **2** and **3**: $E_{2F} = 3.3$ cm^{-1}, $D_{2F} = 13.8$ cm^{-1} ($E_{2F}/D_{2F} = 0.24$) and $E_{3F} = 4.9$ cm^{-1}, $D_{3F} = 15.9$ cm^{-1} ($E_{3F}/D_{3F} = 0.31$).

HF-HFEPR studies: HF-HFEPR studies were carried out for the three complexes at different frequencies (285, 380, and 475 GHz) between $\mu_0 H = 0$ and 12 T on powder samples, pressed into pellets to avoid orientation effects by the applied magnetic field, in a previously described apparatus.[9] For **1**, the spectrum at 285 GHz and $T = 7$ K exhibits one central intense feature with two bands around 5.2 T and three other weaker features around 1.5, 3, and 8 T. The feature at 8 T is doubled like the intense one at 5.2 T (Figure 5, top). The spectrum at 380 GHz has two large bands at 1.6 and 2.5 T (Figure 5, middle), and the spectrum at 475 GHz has two very weak bands at 2.5 and 5.5 T and two intense bands, one around 1 T and the other centered at 8.5 T (Figure 5, bottom). This last band seems to be doubled, like those observed in the spectrum at 285 GHz. Since the magnetization and FDMRS studies suggest that the sign of D is positive for **1** and these data give a good estimation of the anisotropy parameters, we calculated the variation of the spin energy levels versus $\mu_0 H$ [$E(M_S) = f(\mu_0 H)$] along the
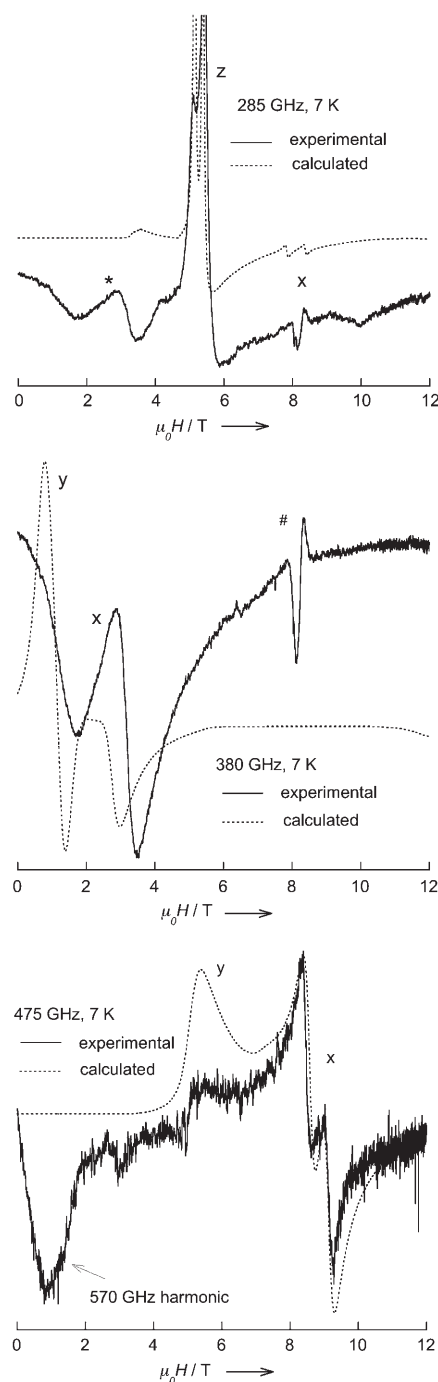

Figure 5. HF-HFEPR spectrum of **1** at T = 7 K; experimental (——) and calculated (-----) at $\nu = 285$ (top), 380 (middle), and 475 GHz (bottom); * corresponds to the 380 GHz harmonics, and # to an artefact.

three canonic directions x, y, and z for $D = +15.9$ cm^{-1} and $E/D = 0.2$; the g value was taken as isotropic and equal to 2.1 (Figure 6). Examination of the three plots allows us to assign the observed bands for the spectrum at 285 GHz. The features around 5.2 T correspond to transitions from a ground level ($M_S = 0$) to a first excited level ($|1>_A$) along the z direction; the feature at 8 T corresponds to the transi-
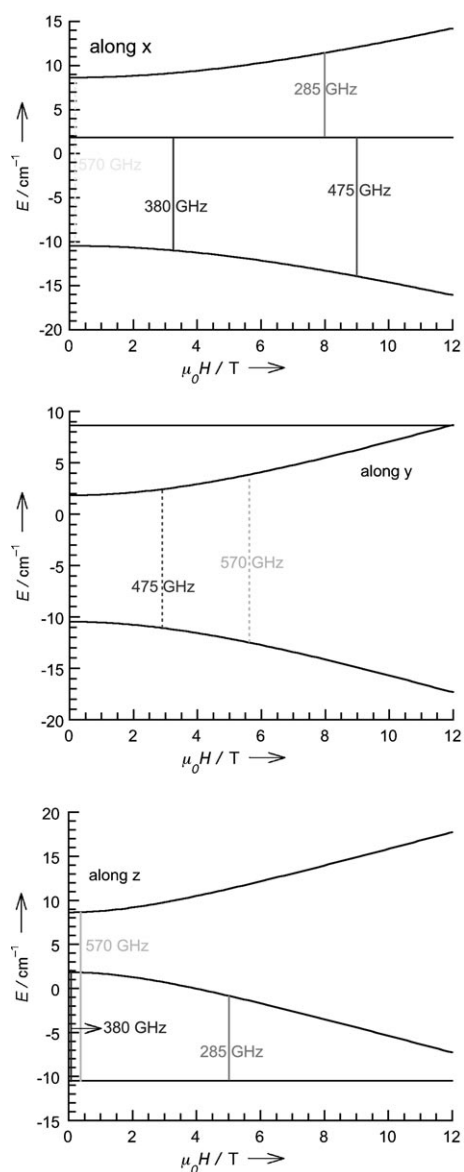
Figure 6. $E(M_S) = f(\mu_0 H)$ for $D = 15.9$ cm^{-1}, $E = 3.2$ ($E/D = 0.2$), and $g = 2.1$ along the directions x (top), y (middle), and z (bottom). The expected transitions for four different frequencies are shown: allowed (——) and "forbidden" (-----).

tion between two excited levels along the x direction. At low temperature, the relative intensities of the two transitions agree with a positive D value; the band at 5.2 T must be more intense than that at 8 T, since it corresponds to a transition from a ground level, as observed experimentally. The sign of D was confirmed by recording the 285 GHz spectrum at $T = 17$ K; the intensity of the transitions at 5.2 T decreases on heating, while that of the transition at 8 T slightly increases (see Figure S4 in the Supporting Information). Along y no allowed transition is expected at 285 GHz within the examined field range. The two remaining bands at 1.5 and 3 T are probably due to contamination of the main 285 GHz wave by higher harmonics (380 GHz). Indeed, two bands stemming from the ground level are ex-

pected at 380 GHz along the z and x directions around 0 and 3 T, respectively. The assignment of the bands for the other two frequencies is straightforward based on the above analysis. A last important point is the doubling of some of the bands in the different spectra. The only reasonable hypothesis was to assume the presence of two species in the compound that differ very slightly from the structural point of view and lead to two distinct signals in the EPR spectra. The EPR spectra were calculated by using a simulation program provided by H. Weihe.[10] A first simulation of the spectra at 285 GHz shows that a slight change in the starting D value, by less than 1%, may lead to two different signals. Furthermore, preliminary simulations taking into account two different species showed that their relative weight is close to unity. Bearing these hypotheses in mind, the spectra were simulated at the three different frequencies by using two different sets (denoted a and b below) of D, E, g_x, g_y, and g_z values. The calculated spectra for each set of parameters were combined under the assumption of equal contributions. The results of the simulation with the best set of parameters are shown in Figure 5 as dashed lines (see Table 1): $D_{1Ea} = 15.7$ cm^{-1}, $E_{1Ea} = 3.4$ cm^{-1} ($E_{1Ea}/D_{1Ea} = 0.216$), $g_{1xa} = 2.10$, $g_{1ya} = 2.05$, $g_{1za} = 2.15$ and $D_{1Eb} = 15.8$ cm^{-1}, $E_{1Eb} = 3.2$ cm^{-1} ($E_{1Eb}/D_{1Eb} = 0.202$), $g_{1xb} = 2.12$, $g_{1yb} = 2.05$, $g_{1zb} = 2.15$. The HF-HFEPR spectra are sensitive to very small structural changes, since the difference in the D values for the two species present in the compound is only around 0.6%.

For complexes **2** and **3**, similar spectra as for **1** were recorded. They were analyzed by the same procedure. For **3**, two species are observed, while for **2** only one species seems to be present, since no doubling of the bands is observed. The spectra for complexes **2** and **3** were simulated (see Figures S5 and S6 in the Supporting Information for **2** and **3**, respectively) and the following parameters were obtained: $D_{2E} = 13.9$ cm^{-1}, $E_{2E} = 3.5$ cm^{-1} ($E_{2E}/D_{2E} = 0.25$), $g_{2x} = 2.13$, $g_{2y} = 2.00$, $g_{2z} = 2.00$; $D_{3Ea} = 16.12$ cm^{-1}, $E_{3Ea} = 5.23$ cm^{-1} ($E_{3Ea}/D_{3Ea} = 0.32$), $g_{3xa} = 2.25$, $g_{3ya} = 2.22$, $g_{3za} = 2.23$ and $D_{3Eb} = 16.35$ cm^{-1}, $E_{3Eb} = 5.22$ cm^{-1} ($E_{3Eb}/D_{3Eb} = 0.32$), $g_{3xb} = 2.25$, $g_{3yb} = 2.22$, $g_{3zb} = 2.23$.

Comparing the magnitude of the anisotropy parameters obtained from the two different techniques HF-HFEPR and FDMRS (Table 1) shows that the D values differ by less than 1% and that the rhombicity is very well estimated from FDMRS for the three complexes. While HF-HFEPR studies reveal in a straightforward manner the presence of the species that differ very slightly, careful examination of the FDMRS spectra of complex **1** shows that it also exhibits a very small doubling of the bands that indicates the presence of the two species observed in the EPR spectra.

Angular overlap calculations: The striking feature of these results is that the spin Hamiltonian parameters are almost independent of the nature of the X ligands linked to the Ni atom. This is surprising since it has already been shown that the nature of the halogen atoms has a dramatic effect on the magnitude of the anisotropy parameters; D may change from -11.43 to $+3.93$ cm^{-1} when replacing Br by Cl in the

tetracoordinate trigonal [Tp*NiX] complexes.[5c] The other interesting feature is the relatively large D values experimentally observed. In the following, we aim at answering two main questions: 1) what is the origin of the relatively large anisotropies in the three complexes and 2) why are the anisotropy parameters very weakly dependent on the nature of the X ligand. To do so, we performed calculations using software based on the angular overlap model (AOM). Standard AOM parameters from the literature were adapted to our complexes and used for the following calculations.[11] The first step consisted of checking whether the calculations can reproduce the experimental spin Hamiltonian parameters for the three complexes. The following values were obtained: $D_{1c} = 15.4$ cm^{-1}, $E_{1c} = 0.4$ cm^{-1}, ($E_{1c}/D_{1c} = 0.03$); $D_{2c} = 12.4$ cm^{-1}, $E_{2c} = 0.6$ cm^{-1}, ($E_{2c}/D_{2c} = 0.05$) and $D_{3c} = -19.0$ cm^{-1}, $E_{3c} = -4.0$ cm^{-1}, ($E_{3c}/D_{3c} = 0.23$).[12] The axial parameters are fairly well reproduced with ranking as found experimentally, that is, $D_{2c} < D_{1c} < D_{3c}$. The rhombicities of **1, 2**, and **3** are poorly reproduced; however, the calculations do lead to higher rhombicity for complex **3** than for **1** and **2**, as for the experimental data. The sign of D for complex **3** was found to be negative, which is not surprising since the experimental E/D value obtained by EPR is very close to the maximum value of 0.33, where the sign of D has no meaning (see Figure S7 in the Supporting Information). From these results, one can assume that the AOM model gives a good insight into the splitting of the ground spectroscopic term. Highly accurate D and E values are not to be expected, but this model will allow different effects to be examined and general conclusions to be drawn on the variation of the anisotropy with some electronic and structural parameters.

Before analyzing the experimental data of the three complexes, we performed preliminary calculations on two model complexes: one with SPy geometry (C_{4v} symmetry) and the other with a geometry very close to TBP (denoted TBP′ in the following, it corresponds to a TBP geometry with the angles between the equatorial ligands set to 115, 115, and 130° instead of 120°). The model complexes have only σ-donor ligands with e_σ parameters taken as the average of those of the amino groups of the *i*Prtacn ligand ($e_\sigma = 4150$ cm^{-1}). The D value for the C_{4v} complex was found to be $+6$ cm^{-1}, while that of the TBP′ species was negative and larger than 100 cm^{-1} in absolute value. This confirms the qualitative argument stated in the introduction that a relatively large anisotropy is expected for pentacoordinate SPy complexes and a huge one for a structure very close to TBP. Furthermore, these calculations give us the order of magnitude of the axial anisotropy for the two extreme geometries.

In the following, the influence of different factors will be examined for model complexes. Since the crystallographic data showed that the structural parameters of the Ni(*i*Prtacn) moiety vary very little for the three complexes and that the Ni–N$_{i\text{Prtacn}}$ bond lengths are not very different, we assumed an averaged e_σ parameter (4150 cm^{-1}) for the three amine atoms for all the model complexes used below. The three N$_{i\text{Prtacn}}$-Ni-N$_{i\text{Prtacn}}$ angles and the three N$_{i\text{Prtacn}}$-Ni-X1

angles were each taken as the average of those of the three complexes. We then examined the influence of different effects while keeping the other structural and electronic parameters unchanged.

To analyze the experimental anisotropy parameters determined above and to answer the questions concerning the magnitude of the D parameters and the quasi-independence on the nature of the X ligands, we proceeded in several steps.

Influence of the N1-Ni-X2 coordination angle: The first step consisted of calculating the D values versus the N1-Ni-X2 angle θ for a model complex with the structural parameters taken as the average of those of **1–3** and considering that the X ligands have only σ-donor effects of the same intensities as the amino groups, and thus allowing the influence of θ alone to be studied. The results depicted in Figure 7 show
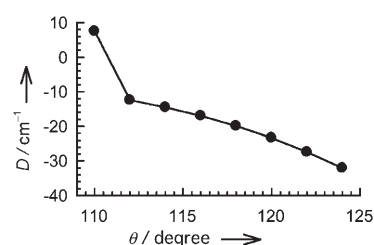

Figure 7. $D = f(\theta)$ for a model complex presenting the average structure of the three complexes, where the same σ-donor effect is considered for the five ligands: $e_\sigma = 4150$ cm^{-1}.

that as expected $|D|$ increases when θ increases and a $|D|$ value of around 23 cm^{-1} is calculated for $\theta = 120°$ (this is the average value of θ for the three complexes). This calculation on a very simple model in which the X ligands are considered as amino groups already leads to a reasonable magnitude for $|D|$. However, at this level, the calculations give negative D values and overestimate the magnitude of the absolute value of D.

Influence of the σ-donor effect of the X ligands in model complexes: To refine our theoretical calculations, we first introduced a distinction in the σ-donor effects between the X atoms and the amino groups. The three curves in Figure 8 show the same general result already observed in Figure 7, that is, $|D|$ increases with increasing θ. The interesting feature of the plots in Figure 8 is that the difference between the $|D|$ values for the three complexes increases with increasing θ. For geometries close to SPy, the $|D|$ values of the three complexes are very close, while for $\theta = 124°$ the nature of the X ligand has a significant influence on the magnitude of $|D|$. For $\theta = 120°$, which corresponds to the average N1-Ni-X2 value of the three complexes, the model predicts a maximum variation of about 20% for $|D|$, which is in good agreement with the 16% variation observed for the experimental D values. Furthermore, the model predicts that $|D_{\text{NCS}}| > |D_{\text{Cl}}| > |D_{\text{Br}}|$, as found experimentally. At this
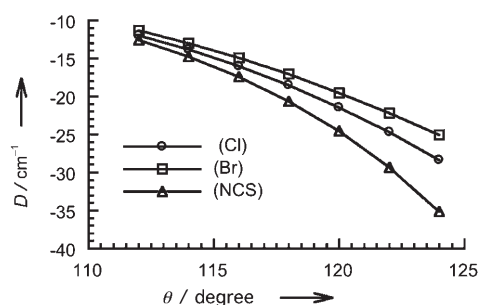
Figure 8. $D = f(\theta)$ for three model complexes each exhibiting the average structure of the three complexes; the amine ligand field is set to the average value of $e_{\sigma}(\text{amine}) = 4150 \text{ cm}^{-1}$ and $e_{\sigma}(X)$ is varied: $e_{\sigma}(\text{Cl}) = 3410 \text{ cm}^{-1}$ (○), $e_{\sigma}(\text{Br}) = 2858 \text{ cm}^{-1}$ (□), and $e_{\sigma}(\text{NCS}) = 4970 \text{ cm}^{-1}$ (△).

level of approximation, the calculations always lead to negative D values for the three complexes with a relatively large rhombicity ($E/D \approx 0.22$, very close to the experimental data).

Influence of the π effect of ligands in model complexes: When the π effect of the X ligands is introduced (Figure 9), three important observations can be made. Firstly, the sign
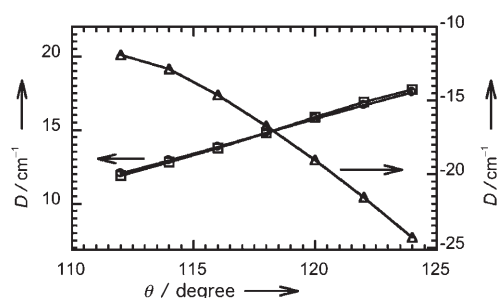

Figure 9. $D = f(\theta)$ for three model complexes with the same parameters as for Figure 8 and considering in addition an average σ effect: $e_{\pi}(\text{Cl}) = 1573 \text{ cm}^{-1}$ (○), $e_{\pi}(\text{Br}) = 1311 \text{ cm}^{-1}$ (□), and $e_{\pi}(\text{NCS}) = 637 \text{ cm}^{-1}$ (△).

of the axial parameters is now found to be positive for **1** and **2**, as observed experimentally, and the experimental rhombicity is very well reproduced (the calculated E/D value for the three complexes is around 0.23). Secondly, a decrease of around 20% in the $|D|$ values for the three complexes is observed, and agreement with the experimental data is very good for **1** and **2** ($D_{1c} = 16.3$ and $D_{2c} = 14.8 \text{ cm}^{-1}$ for $\theta = 121.5$ and 118.2°, respectively, in comparison to experimental values of 15.7 and 13.9 cm^{-1} for **1** and **2**, respectively). However, the value for complex **3** is still negative and overestimated in absolute value (-20 cm^{-1} as opposed to 16.2 cm^{-1} found experimentally for **3**). Thirdly, the π effect of the ligands does not significantly affect the difference between the $|D|$ values of the three complexes.

To gain more insight into the variation of the anisotropy with the structural and electronic parameters θ, e_{σ} and e_{π}, we carried out a series of calculation in which θ and e_{π}/e_{σ} were varied.[13] The results are illustrated in the 3D plot in

Figure 10. This plot has three regions. The first region (A) is a quasiplateau with positive D values; the results for model complexes corresponding to **1** and **2** belong to this area
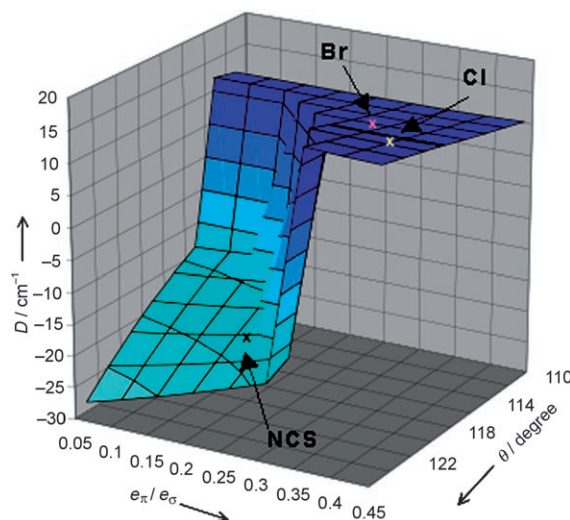

Figure 10. $D = f(\theta, e_{\pi}/e_{\sigma})$ for a model complex exhibiting the average structure of **1**–**3** with $e_{\sigma}(\text{amine}) = 4150 \text{ cm}^{-1}$ and $e_{\sigma}(X) = 3746 \text{ cm}^{-1}$.

where changes in the parameters do not dramatically affect the magnitude and nature of the magnetic anisotropy. The second region (B) is much steeper than A with negative D values, and the third region (C) corresponds to the area where D changes its sign. The result corresponding to the parameters of complex **3** belong to region B and is very close to the border between B and C; thus, a very slight change in the structural parameters will induce a large change in the calculated anisotropy parameters. That explains why for complex **3** the AOM parameters must be estimated very accurately to reproduce the sign of D.

This theoretical study predicts that for a e_{π}/e_{σ} ratio larger than 0.22, a positive D value of around 17 cm^{-1} is expected for angles θ varying between 110 and 125°. On the other hand, for a e_{π}/e_{σ} ratio smaller than 0.15, Ising-type (negative D value) anisotropy is expected, and its magnitude increases with increasing θ.

Influence of the position of the X ligands in a model SPy complex: The last issue to be rationalized is the relatively small difference in the D values between complexes **1** and **2** when compared to the tetracoordinate Ni^{II} complexes [Ni(PPh$_3$)$_2$X$_2$] and [Tp*NiX]. Our hypothesis is that, for the general case of pentacoordinate complexes with a geometry close to SPy and halogen atoms in the coordination sphere of the metal ion, the position of the halo ligands (apical or equatorial) may have a large effect on the magnitude of the axial anisotropy. To check this assumption, we carried out two series of calculation on SPy model complexes. In the first we considered a complex of formula NiL$_3$X$_2$ where the two X ligands were fixed in equatorial positions and their e_{σ} values were varied (the e_{σ} value of the L ligands was set to
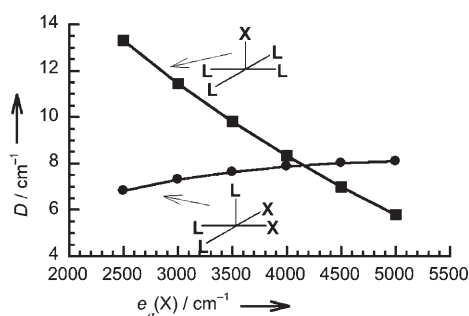
Figure 11. $D = f[e_\sigma(X)]$ for square pyramidal complexes NiL_4X and $[NiL_3X_2]$ with $e_\sigma(L) = 4150$ cm^{-1}: X at the equatorial positions for NiL_3X_2 (●) and at the apical position for NiL_4X (■).

4150 cm^{-1}, corresponding to that of the amine ligands in model complexes). The results depicted in Figure 11 show that doubling $e_\sigma(X)$ (from 2500 to 5000 cm^{-1}) leads to an increase of 20% for D. This is in line with the difference experimentally found for **1** and **2**. The second series of calculations was carried out on a SPy complex of formula NiL_4X where X is the apical ligand. In such a case, a decrease of 60% in the D value occurs. Thus, a change in the σ-donor effect of the apical ligand has a dramatic effect on the magnitude of the axial anisotropy, while in the case of equatorial ligands it has almost no effect. These results rationalize the experimental data concerning the magnitude of the axial anisotropy in complexes **1** and **2**, and show that, for an SPy geometry, the axial magnetic anisotropy is mainly governed by the position of the X ligands in the coordination sphere of the metal ion.

Conclusion

A macrocyclic tridentate triazacyclononane bearing isopropyl groups (*i*Prtacn) imposes a structural environment around Ni^{II} that leads to pentacoordinate complexes of general formula [Ni(*i*Prtacn)X$_2$] with similar molecular structures. Despite the difference in the electronic nature of the X ligands (X = Cl, Br, NCS), the axial anisotropy obtained from FDMRS and HF-HFEPR studies is the same for the three complexes to within about 10%. Analysis of the different effects induced by the ligands on model complexes led to the conclusion that the axial anisotropy is expected to be large for such complexes and depends mainly on the geometrical structure and not much on the electronic structure of the X ligands. This weak dependence on the nature of the X ligand occurs mainly for geometries that are close to SPy and only when these ligands are in the equatorial positions of the square pyramid, as is the case for the present complexes. These results mean that, for pentacoordinate Ni^{II} complexes, 1) *i*Prtacn imposes a structure that leads to axial anisotropy confined in a narrow range of magnitude and 2) the nature of the ligands that can be chemically substituted has little effect on the magnitude of the anisotropy. Calculations on a hypothetical complex with bidentate oxalate

($C_2O_4^{2-}$) ligand in place of the two X atoms gives a D value of 20 cm^{-1},[14] while a value of 1.5 cm^{-1} was obtained (experimentally and by calculation) for the hexacoordinate [Ni(bpy)$_2$(C$_2$O$_4$)] (bpy = 2,2′-bipyridine).[15] Thus the Ni(*i*Prtacn) moiety induces, in pentacoordinate complexes, a "stable" magnetic anisotropy that is almost independent of the remaining two ligands. This makes complexes based on the Ni(*i*Prtacn) unit ideal building blocks for introducing huge local magnetic anisotropy into polynuclear species and/or coordination networks.

Experimental Section

[Ni(*i*Prtacn)Br$_2$] (2): NiBr$_2$·6H$_2$O (0.65 g, 2×10^{-3} mol) was dissolved in methanol (10 mL). DME (30 mL), THF (100 mL), and methyl orthoformate (2 mL) were added to this solution, and the mixture was refluxed for 10 min to give a deep purple solution. Then, a solution of *i*Prtacn (0.5 g, 2×10^{-3} mol) in THF (20 mL) was added dropwise. A change of color from purple to yellow was observed just before a microcrystalline solid precipitated. The vessel was left to cool and the powder was collected by filtration, thoroughly washed with THF, and dried under vacuum. Purification can be performed by dissolution in chloroform, filtration to remove impurities, and reprecipitation in THF. Elemental analysis (%) calcd for C$_{15}$H$_{33}$Br$_2$N$_3$Ni: C 46.79, H 7.02, N 8.87, Br 33.72, Ni 12.38; found: C 46.45, H 7.27, N 8.87, Br 33.42, Ni 12.00.

[Ni(*i*Prtacn)(NCS)$_2$] (3): [Ni(*i*Prtacn)Br$_2$] (0.1 g, 2×10^{-4} mol) was dissolved in methanol (20 mL) and two molar equivalents of NaNCS (32.4 mg) dissolved in methanol (10 mL) were added dropwise. The color of the solution changed from yellow to blue and a microcrystalline solid precipitated. It was collected by filtration, washed with small amounts of cold methanol, and dried under vacuum. Elemental analysis (%) calcd for C$_{17}$H$_{33}$N$_5$NiS$_2$: C 47.45, H 7.73, N 16.28, S 14.90, Ni 13.64; found: C 47.32, H 7.61, N 16.26, S 14.81, Ni 13.30.

Crystallographic studies: X-ray diffraction data for **1–3** were collected on a Kappa X8 APPEX II Bruker diffractometer with graphite-monochromated Mo$_{K\alpha}$ radiation ($\lambda = 0.71073$ Å). The data were corrected for Lorentzian, polarization, and absorption effects. The structures were solved by direct methods using SHELXS-97 and refined against F^2 by full-matrix least-squares techniques using SHELXL-97 with anisotropic displacement parameters for all non-hydrogen atoms.[16] Hydrogen atoms were located on a difference Fourier map and introduced into the calculations in a riding model with isotropic thermal parameters. All calculations were performed by using the Crystal Structure crystallographic software package WINGX.[17] The crystal data for the three complexes can be found in the Supporting Information.

CCDC-656604, CCDC-656605 and CCDC-656606 contain the supplementary crystallographic data for this paper. These data can be obtained free of charge from The Cambridge Crystallographic Data Centre via www.ccdc.cam.ac.uk/data_request/cif.

Magnetization studies: Magnetization measurements were performed on 5 mg pressed pellets in the 0–5 T range at 2,3, 4 and 6 K using a Quantum Design MPMS5 SQUID magnetometer.

FDMRS: FDMRS measurements were performed on a spectrometer described in the literature.[18] Spectra were recorded on a pressed powder pellet of 155 mg with a diameter of 1 cm and a thickness of 1.82 mm at various temperatures.

HF-HFEPR: EPR experiments were performed at the High Magnetic Field Laboratory, Grenoble, France, using a previously described apparatus.[9] Ground crystals (about 100 mg for EPR and 5 mg for SQUID) pressed to form a pellet in order to reduce torquing under high magnetic fields were used. The simulation program is available from Dr. H. Weihe; for more information see http://sophus.kiku.dk/software/epr/epr.html.[10]

[1] a) A. L. Barra, L.-C. Brunel, D. Gatteschi, L. Pardi, R. Sessoli, *Acc. Chem. Res.* **1998**, *31*, 460; b) A.-L. Barra, A. Caneschi, A. Cornia, A. F. Fabrizi de Biani, C. Fabretti, D. Gatteschi, C. Sangregorio, R. Sessoli, L. Sorace, *J. Am. Chem. Soc.* **1999**, *121*, 5302; c) A. Caneschi, D. Gatteschi, N. Lalioti, C. Sangregorio, R. Sessoli, G. Venturi, A. Vindigni, A. Rettori, M. G. Pini, M. A. Novak, *Angew. Chem.* **2001**, *113*, 1810–1813; *Angew. Chem. Int. Ed.* **2001**, *40*, 1760; d) R. Clerac, H. Miyasaka, M. Yamashita, C. Coulon, *J. Am. Chem. Soc.* **2002**, *124*, 12837; e) R. Lescouëzec, J. Vaissermann, C. Ruiz-Perez, F. Lloret, R. Carrasco, M. Julve, M. Verdaguer, Y. Dromzee, D. Gatteschi, W. Wernsdorfer, *Angew. Chem.* **2003**, *115*, 1521; *Angew. Chem. Int. Ed.* **2003**, *42*, 1483; f) D. Collison, M. Murrie, V. S. Oganesyan, S. Piligkos, N. R. J. Poolton, G. Rajaraman, G. M. Smith, A. J. Thompson, G. A. Timko, W. Wernsdorfer, R. E. P. Winpenny, E. J. McInnes, *Inorg. Chem.* **2003**, *42*, 5293; g) L. M. C. Beltran, J. R. Long, *Acc. Chem. Res.* **2005**, *38*, 325–334; h) S. J. Langley, M. Helliwell, R. Sessoli, P. Rosa, W. Wernsdorfer, R. E. P. Winpenny, *Chem. Commun.* **2005**, 5029; i) S. Accorsi, A.-L. Barra, A. Caneschi, G. Chastanet, A. Cornia, A. C. Fabretti, D. Gatteschi, C. Mortalo, E. Olivieri, F. Parenti, P. Rosa, R. Sessoli, L. Sorace, W. Wernsdorfer, L. Zobbi, *J. Am. Chem. Soc.* **2006**, *128*, 4742; j) J. N. Rebilly, T. Mallah, *Struct. Bonding (Berlin)* **2006**, *122*, 103; k) D. Brinzei, L. Catala, C. Mathonière, W. Wernsdorfer, A. Gloter, O. Stephan, T. Mallah, *J. Am. Chem. Soc.* **2007**, *129*, 3778.

[2] O. Kahn, *Molecular Magnetism*, VCH, Weinheim, **1993**.

[3] F. E. Mabbs, D. Collison in *Electron Paramagnetic Resonance of d Transition Metal Compounds*, Elsevier, Amsterdam, **1992**, pp. 480.

[4] a) R. Boca, *Coord. Chem. Rev.* **2004**, *248*, 757–815, and references therein; b) G. Rogez, J. N. Rebilly, A. L. Barra, L. Sorace, G. Blondin, N. Kirchner, M. Duran, J. van Slageren, S. Parsons, L. Ricard, A. Marvilliers, T. Mallah, *Angew. Chem.* **2005**, *117*, 1910; *Angew. Chem. Int. Ed.* **2005**, *44*, 1876; c) D. Dobrzynska, L. B. Jerzykiewicz, M. Duczmal, A. Wojciechowska, K. Jablonska, J. Palus, A. Ozarowski, *Inorg. Chem.* **2006**, *45*, 10479; d) J. Titis, R. Boca, L. Dlhan, T. Durcekova, H. Fuess, R. Ivanikova, V. Mrazova, I. Svoboda, *Polyhedron* **2007**, *26*, 1523.

[5] a) J. Krzystek, J. H. Park, M. W. Meisel, M. A. Hitchman, H. Stratemeier, L. C. Brunel, J. Telser, *Inorg. Chem.* **2002**, *41*, 4478–4487; b) S. Vongtragool, B. Gorshunov, M. Dressel, J. Krzystek, D. M. Eichhorn, J. Telser, *Inorg. Chem.* **2003**, *42*, 1788; c) P. J. Desrochers, J. Telser, S. A. Zvyagin, A. Ozarowski, J. Krzystek, D. A. Vicic, *Inorg. Chem.* **2006**, *45*, 8930.

[6] a) G. Haselhorst, S. Stoetzel, A. Strassburger, W. Walz, K. Wieghardt, B. Nuber, *J. Chem. Soc. Dalton Trans.* **1993**, 83; b) J. N. Rebilly, L. Catala, E. Riviere, R. Guillot, W. Wernsdorfer, T. Mallah, *Inorg. Chem.* **2005**, *44*, 8194.

[7] Selected bond lengths [Å] and angles [°] for **1**: Ni−N1 2.0829(17), Ni−N2 2.1883(17), Ni−N3 2.1346(17), Ni−Cl1 2.3914(6), Ni−Cl2 2.2870(6); N1-Ni-N2 85.23(6), N1-Ni-N3 86.89(6), N1-Ni-Cl1 93.37(5), N1-Ni-Cl2 121.52(5), N2-Ni-N3 82.77(6), N2-Ni-Cl1 176.38(4), N2-Ni-Cl2 93.10(5), N3-Ni-Cl1 93.83(5), N3-Ni-Cl2 150.98(5), Cl1-Ni-Cl2 90.48(2). For **2**: Ni−N1 2.080(3), Ni−N2 2.208(3), Ni−N3 2.127(3), Ni−Br1 2.5480(8), Ni−Br2 2.4615(8); N1-Ni-N2 85.24(12), N1-Ni-N3 87.43(13), N1-Ni-Br1 94.73(9), N1-Ni-Br2 118.20(9), N2-Ni-N3 81.80(12), N2-Ni-Br1 177.50(8), N2-Ni-Br2 93.54(9), N3-Ni-Br1 95.69(9), N3-Ni-Br2 153.62(9), Br1-Ni-Br2 88.68(3). For **3**: Ni−N1 2.068(2), Ni−N2 2.152(2), Ni−N3 2.114(2), Ni−N1B 2.014(3), Ni−N2A 1.982(3); N1-Ni-N2 86.28(10), N1-Ni-N3 87.18(9), N1-Ni-N1B 92.94(12), N1-Ni-N2A 121.36(11), N2-Ni-N3 83.46(9), N2-Ni-N1B 177.75(10), N2-Ni-N2A 93.32(11), N3-Ni-N1B 94.39(10), N3-Ni-N2A 151.11(11), N1B-Ni-N2A 88.90(12).

[8] N. Kirchner, J. van Slageren, M. Dressel, *Inorg. Chim. Acta* **2007**, DOI: 10.1016/j.ica.2007.01.013.

[9] A.-L. Barra, L.-C. Brunel, J. B. Robert, *Chem. Phys. Lett.* **1990**, *165*, 107.

[10] J. Glerup, H. Weihe, *Acta Chem. Scand.* **1991**, *45*, 444.

[11] a) A. B. P. Lever, *Inorganic Electronic Spectroscopy*, Elsevier, Amsterdam, **1984**; b) A. Bencini, I. Ciofini, M. G. Uytterhoeven, *Inorg. Chim. Acta* **1998**, *274*, 90; c) A. Bencini, C. Benelli, D. Gatteschi, *Coord. Chem. Rev.* **1984**, *60*, 131; d) I. Bertini, D. Gatteschi, A. Scozzafava, *Inorg. Chem.* **1976**, *15*, 203; e) A. B. P. Lever, I. M. Walker, P. J. McCarthy, K. B. Mertes, A. Jircitano, R. Sheldon, *Inorg. Chem.* **1983**, *22*, 2252; f) L. Y. Martin, C. Robert Sperati, D. H. Bush, *J. Am. Chem. Soc.* **1977**, *99*, 3778; g) R. J. Deeth, M. Gerloch, *Inorg. Chem.* **1987**, *26*, 2582; h) R. Stranger, S. C. Wallis, L. R. Gahan, C. H. L. Kennard, K. A. Byriel, *J. Chem. Soc. Dalton Trans.* **1992**, 2971.

[12] Racah parameters for the Ni^{II} ion: $B = 860$ cm^{-1}, $C = 3350$ cm^{-1}, $\zeta = 600$ cm^{-1}. Parameters for **1**: $e_\sigma(N1) = 4628$ cm^{-1}, $e_\sigma(N2) = 3671$ cm^{-1}, $e_\sigma(N3) = 4150$ cm^{-1}, $e_\sigma(Cl1) = 3029$ cm^{-1}, $e_\pi(Cl1) = 1244$ cm^{-1}, $e_\sigma(Cl2) = 3792$ cm^{-1}, $e_\pi(Cl2) = 1628$ cm^{-1}; parameters for **2**: $e_\sigma(N1) = 4729$ cm^{-1}, $e_\sigma(N2) = 3508$ cm^{-1}, $e_\sigma(N3) = 4219$ cm^{-1}, $e_\sigma(Br1) = 2613$ cm^{-1}, $e_\pi(Br1) = 900$ cm^{-1}, $e_\sigma(Br2) = 3102$ cm^{-1}, $e_\pi(Br2) = 1106$ cm^{-1}; parameters for **3**: $e_\sigma(N1) = 4868$ cm^{-1}, $e_\sigma(N2) = 3989$ cm^{-1}, $e_\sigma(N3) = 4361$ cm^{-1}, $e_\sigma(N1B) = 4898$ cm^{-1}, $e_\pi(N1B) = 1076$ cm^{-1}, $e_\sigma(N2A) = 5040$ cm^{-1}, $e_\pi(N2A) = 605$ cm^{-1}. Evaluation of the parameters of NCS$^-$ is not easy because the Ni-N-C angle can deviate from linearity and because of the conjugated π-donor and π-acceptor effects of this ligand. The AOM parameters used for NCS were taken from complexes that have the same Ni-N-C angles as **3**.[11g]

[13] To determine how the structural and electronic effects combine to determine the magnetic anisotropy, we should analyze the anisotropy as a function of θ, e_σ, and e_π. As the variation of D with e_σ is slightly slower than that with θ, we chose to simplify the analysis by carrying out a series of calculation in which θ and e_π/e_σ were varied, while e_σ was maintained at a constant value.

[14] For the three complexes, the X1-Ni-X2 angles are around 90°. The structure of the hypothetical [Ni(iPrtacn)(oxalate)] was fixed to that of the average model complex already used, apart from the O-Ni-O bite angle of the oxalate, which was fixed at 80°, as is experimentally the case, instead of around 90° as found for the X1-Ni-X2 angles of complexes **1**–**3**. The calculations were done with the following parameters for the oxygen atoms of the oxalate ligand: $e_\sigma = 4355$ cm^{-1} and $e_\pi = 1355$ cm^{-1}.

[15] G. Rogez, PhD thesis, Université Paris 11, **2002**. The spin Hamiltonian parameters for [Ni(bpy)$_2$(C$_2$O$_4$)] were determined from HF-HFEPR studies ($D = -1.44$ cm^{-1} and $E/D = 0.04$).

[16] a) G. M. Sheldrick, SHELXS-97, Program for crystal structure solution, University of Göttingen, Göttingen, Germany, **1990**; b) G. M. Sheldrick, SHELXL-97, Program for the refinement of crystal structures from diffraction data, University of Göttingen, Göttingen, Germany, **1997**.

[17] L. J. Farrugia, *J. Appl. Crystallogr.* **1999**, *32*, 837.

[18] J. van Slageren, S. Vongtragool, B. Gorshunov, A. A. Mukhin, N. Karl, J. Krzystek, J. Telser, A. Müller, C. Sangregorio, D. Gatteschi, M. Dressel, *Phys. Chem. Chem. Phys.* **2003**, *5*, 3837.